BBA - Molecular Basis of Disease 1864 (2018) 660–667

Contents lists available at ScienceDirect

BBA - Molecular Basis of Disease

journal homepage: www.elsevier.com/locate/bbadis

Factor VII deficiency: Unveiling the cellular and molecular mechanisms underlying three model alterations of the enzyme catalytic domain

Maria Eugenia Chollet[a,b,c,*], Elisabeth Andersen[a,b,c], Ellen Skarpen[d], Christiane F. Myklebust[a,b], Christian Koehler[e], Jens Preben Morth[f,g], Ampaiwan Chuansumrit[h], Mirko Pinotti[i], Francesco Bernardi[i], Bernd Thiede[e], Per Morten Sandset[a,b,c], Grethe Skretting[a,b]

[a] Department of Hematology, Oslo University Hospital, NO-0424 Oslo, Norway
[b] Research Institute of Internal Medicine, Oslo University Hospital, NO-0424 Oslo, Norway
[c] Institute of Clinical Medicine, University of Oslo, Oslo, Norway
[d] Core facility for Advanced Light Microscopy, Institute for Cancer Research, Oslo University Hospital, NO-0379 Oslo, Norway
[e] Department of Biosciences, University of Oslo, NO-0316 Oslo, Norway
[f] Center for Molecular Medicine Norway (NCMM), Nordic EMBL Partnership University of Oslo, NO-0349 Oslo, Norway
[g] Institute for Experimental Medical Research, Oslo University Hospital, N-0424 Oslo, Norway
[h] Department of Pediatrics, Mahidol University, Bangkok, Thailand
[i] Department of Life Sciences and Biotechnology, University of Ferrara, Ferrara, Italy

ARTICLE INFO

Keywords:
Factor VII
Factor VII deficiency
Mutations
Protein trafficking
ER retention

ABSTRACT

Activated factor (F) VII is a vitamin K-dependent glycoprotein that initiates blood coagulation upon interaction with tissue factor. FVII deficiency is the most common of the rare congenital bleeding disorders. While the mutational pattern has been extensively characterized, the pathogenic molecular mechanisms of mutations, particularly at the intracellular level, have been poorly defined. Here, we aimed at elucidating the mechanisms underlying altered FVII biosynthesis in the presence of three mutation types in the catalytic domain: a missense change, a microdeletion and a frameshift/elongation, associated with severe or moderate to severe phenotypes. Using CHO-K1 cells transiently transfected with expression vectors containing the wild-type FVII cDNA (FVIIwt) or harboring the p.I289del, p.G420V or p.A354V-p.P464Hfs mutations, we found that the secretion of the FVII mutants was severely decreased compared to FVIIwt. The synthesis rate of the mutants was slower than the FVIIwt and delayed, and no degradation of the FVII mutants by proteasomes, lysosomes or cysteine proteases was observed. Confocal immunofluorescence microscopy studies showed that FVII variants were localized into the endoplasmic reticulum (ER) but were not detectable within the Golgi apparatus. These findings suggested that a common pathogenic mechanism, possibly a defective folding of the mutant proteins, was triggered by the FVII mutations. The misfolded state led to impaired trafficking of these proteins causing ER retention, which would explain the low to very low FVII plasma levels observed in patients carrying these mutations.

1. Introduction

Inherited factor (F) VII deficiency is the most common among rare congenital bleeding disorders with an estimated prevalence of between 1:300,000 and 1:500,000 [1,2]. It has an autosomal recessive pattern of inheritance and clinically it varies ranging from lethal to mild bleeding or even asymptomatic forms [2–4]. The mutational pattern of the *F7* gene is heterogeneous (see http://www.hgmd.cf.ac.uk/ac/index.php). Between 70 and 80% of the disease-associated mutations are represented by missense mutations associated with reduced FVII plasma levels in patients [3]. The remainder is caused by nonsense mutations, deletions, or splicing site changes [5]. Even though the mutational pattern of FVII deficiency is well characterized and the functional aspects of some of the mutant FVII proteins have been explored, the role of intracellular processing of mutant FVII molecules has only been investigated for a few mutations [6–9]. A nonsense mutation in the carboxy-terminal FVII domain induced an impaired secretion of the mutant protein with retention in the endoplasmic reticulum (ER), which demonstrated that the carboxy-terminal region of FVII is essential for FVII secretion [9]. In another report a compound heterozygous point mutation in the central hydrophobic core of the signal peptide and nonsense mutation in the carboxy-terminal domain, induced defective

* Corresponding author at: Research Institute of Internal Medicine, Oslo University Hospital Rikshospitalet, Box 4950, Nydalen, NO-0424 Oslo, Norway.
E-mail address: Maria.Eugenia.Chollet.Dugarte@rr-research.no (M.E. Chollet).

https://doi.org/10.1016/j.bbadis.2017.12.016
Received 31 August 2017; Received in revised form 24 November 2017; Accepted 11 December 2017
Available online 12 December 2017
0925-4439/ © 2017 Elsevier B.V. All rights reserved.

trafficking of the mutant FVII with retention in ER and extensive intracellular degradation [8].

It is known that in eukaryotic cells nearly one third of the newly synthesized proteins are targeted to the ER, which represents the first step in the transport of these proteins to other organelles or to the extracellular space [10]. In the ER the folding of nascent proteins and post-translational modifications, which are important steps for proper folding and function of the proteins, are guided by resident enzymes and molecular chaperones [10–12]. Since only correct folded proteins can leave the ER, proteins that fail to adopt their native state are retained and eventually targeted for ER-associated degradation [11,13,14].

For other blood coagulation disorders, it was previously shown that mutations may cause either impaired transport of the protein from the ER to the Golgi [15] or excessive intracellular degradation [16,17]. Accordingly, the molecular mechanisms underlying the functional effect of the various mutant proteins causing blood coagulation disorders can differ between the genetic defects. Therefore, the aim of the present study was to characterize three types of mutations (p.G420V, p.I289del and A354V-p.P464Hfs) in the FVII catalytic domain in order to unveil the molecular mechanisms responsible for FVII deficiency. The p.G420V missense change is associated with undetectable FVII protein levels in plasma and severe bleeding [7]. The one-residue deletion p.I289del was found in a patient who presented severe intra-cranial bleeding at birth and undetectable levels of FVII protein in plasma (Pinotti M, Chuansumrit A, unpublished). The frame-shifted elongated variant p.A354V-p.P464Hfs, has a phenotype that ranges from asymptomatic to moderate and severe bleedings. Using CHO-K1 cells overexpressing either the FVII wild type (FVIIwt) or one of the mutants, we investigated in vitro the molecular and cellular mechanisms by which these mutations may decrease the FVII levels in the plasma of the patients. We found that the synthesis of the mutant proteins was slow and delayed and their secretion was severely affected. This indicates a possible retention of the mutant proteins in the ER resulting in impaired trafficking.

2. Material and methods

2.1. Cell cultures

Chinese hamster ovary cells (CHO-K1) were obtained from the American Type Culture Collection (ATCC®CCL-61, Rockville, MD, USA). Cells were maintained at 37 °C in a humidified atmosphere with 5% CO_2 in Dulbecco's Modified Eagles Medium (DMEM, Lonza, Verviers, Belgium) supplemented with 10% fetal bovine serum (FBS, HyClone Thermo Scientific, Northumberland, UK), 100 IU/mL penicillin and 100 μg/mL streptomycin (Lonza).

2.2. Construction of expression vectors and transfections

A plasmid expressing FVIIwt was generated in pcDNA™ $3.1^{(+)}$ (Thermo Fisher Scientific Inc., Waltham, MA, USA) as described previously [7] and named pcDNA3-FVIIwt. To create plasmids expressing FVII variants, mutations were introduced into pcDNA3-FVIIwt using the Quick-Change site directed mutagenesis kit (Stratagen-Agilent, La Jolla, CA, USA) as described elsewhere [1,7]. For transient transfections, CHO-K1 cells were grown in 6-well plates until 80% confluency. Vitamin K1 (Sigma Aldrich, Saint Louis, MO, USA), 10 μg/mL, was then added to the medium and the cells were transfected with 2.5 μg of pcDNA3-FVIIwt, pcDNA3-p.G420V, pcDNA3-p.I289del, or pcDNA3-p.A354V-p.P464Hfs using Lipofectamine LTX Plus (Thermo Fisher Scientific) following the manufacturer's instructions. To generate cells stably expressing the FVII variants, CHO-K1 cells were grown in complete DMEM medium supplemented with 800 μg/mL of Geneticine (G-418 Thermo Fisher Scientific) for three weeks. Clones were tested for expression of FVII using quantitative RT-PCR and the clones with highest mRNA expression levels were isolated and expanded. The cell lines were maintained in complete DMEM containing 400 μg/mL of Geneticine.

2.3. Quantitative RT-PCR (qRT-PCR)

Twenty-four hour post transfection total mRNA was isolated using the MagMAX™-96 Total RNA Isolation Kit on a MagMAX™ Express-96 Deep Well Magnetic Particle Processor (both from Thermo Fisher Scientific). mRNA was reversely transcribed using the High Capacity cDNA Reverse Transcription kit (Thermo Fisher Scientific). FVII mRNA levels were determined by the 7900HT Fast Real-Time PCR system (Thermo Fisher Scientific) using a TaqMan Gene Expression Assay for FVII (Hs01551992_m1, Thermo Fisher Scientific) according to the manufacturer's instructions. TATA binding protein (TBP, Hs99999910_m1, Thermo Fisher Scientific) was used as endogenous control, and the Ct values of the target gene was normalized against the endogenous control cDNA. Relative mRNA level was calculated using the comparative threshold method ($2^{-\Delta\Delta Ct}$).

2.4. FVII expression levels

Twenty-four hour post transfection the culture medium was collected and the cells were washed three times with pre-chilled phosphate-buffered saline (PBS). The cells were lysed in RIPA buffer (Sigma Aldrich) containing Halt protease and phosphatase inhibitor cocktail 1X (Thermo Fisher Scientific). FVII antigen (FVIIAg) was measured in cell lysates and culture medium using the Visualize FVII antigen ELISA kit (Affinity Biologicals Inc., Ancaster, ON, Canada). Total protein concentrations in the lysates were measured using the BCA Protein Assay kit (Thermo Fisher Scientific) and FVIIAg levels were normalized against the total protein concentration of the corresponding cell lysates. Three independent experiments in duplicates were performed. FVII activity in the medium was determined using the Human FVII Chromogenic Activity Kit (Nordic BioSite AB, Täby, Sweden) according to manufacturer's instructions.

2.5. Synthesis and stability of FVII by pulse chase stable isotope labeling with amino acids in cell culture (pc-SILAC)

CHO-K1 cells were grown in SILAC DMEM medium supplemented with 10% FBS for SILAC, L-lysine 2HCL and L-arginine HCL (all from Thermo Fisher Scientific) (light medium). Proline (Thermo Fisher Scientific) was added to the medium at 200 mg/L. Cells were cultured in this pre-exchange light (L) medium until a minimum of three divisions were reached. Cells were then seeded in 6-well plates and cultured in DMEM light (L) medium until 80% confluency. After 24 h, cells were transiently transfected with pcDNA3-FVIIwt, pcDNA3-p.G420V, pcDNA3-p.I289del, or pcDNA3-p.A354V-p.P464Hfs as described above. Four hours after transfection, the light (L) medium was exchanged for heavy (H) medium containing $^{13}C_6$ $^{15}N_4$ L-arginine, $^{13}C_6$ $^{15}N_2$ L-lysine and proline at 200 mg/L (Thermo Fisher Scientific) for cells transfected with pcDNA3-FVIIwt. For cells transfected with pcDNA3-p.G420V, pcDNA3-p.I289del, or pcDNA3-p.A354V-p.P464Hfs, the light (L) medium was exchanged for medium containing $^{13}C_6$- L-arginine, L-lysine 2HCL (4,4,5,5-D4) and proline 200 mg/L (medium medium M) (Thermo Fisher Scientific). 0, 1, 2, 4, 6, 24, and 48 h after exchange of medium the cells were harvested, washed with pre-chilled PBS (Lonza) and lysed with RIPA buffer containing Halt protease and phosphatase inhibitor cocktail 1X (Thermo Fisher Scientific). Cell lysates, were collected at each time point of FVIIwt (heavy) or the FVII mutants (medium) and were mixed at equal proportions. Proteins were separated by SDS-PAGE using Mini-PROTEAN® TGX™ 10% Precast Gels (Bio-Rad, Hercules, CA, USA) and stained with Coomassie Blue (Bio-Rad). For the liquid chromatography-mass spectrometry (LC-MS), the gel bands were excised and in-gel digestion was carried out with 0.1 μg

trypsin (Promega, Madison, WI, USA) in 20 µL 25 mM NH_4HCO_3 pH 7.8, 1 mM $CaCl_2$, for 16 h at 37 °C. The peptides were purified with µ-C18 ZipTips (Millipore, Billerica, MA, USA), dried in a Speed Vac concentrator and dissolved in 10 µL of 1% formic acid. The tryptic peptides were analyzed using an Ultimate 3000 nano-UHPLC system (Dionex, Sunnyvale, CA, USA) connected to a Q Exactive mass spectrometer (ThermoElectron, Bremen, Germany) equipped with a nanoelectrospray ion source. For separation of the peptides by liquid chromatography, an Acclaim PepMap 100 column (50 cm × 75 µm) packed with 100 Å C18 3 µm particles (Dionex) was used. A flow rate of 300 nL min^{-1} was employed with a solvent gradient of 3–35% B in 42 min, to 50% B in 8 min and then to 80% B in 2 min. Solvent A was 0.1% formic acid and solvent B was 0.1% formic acid/90% acetonitrile. The mass spectrometer was operated in a mode switching between targeted SIM scans (tSIM) and targeted MS2 scans (tMS2/PRM) following a reference library containing the 12 target masses for four light (L), medium (M) and heavy (H) labeled peptides and their retention times. tSIM scans were acquired using an isolation window of 2 Th (Th is a unit of the mass-to-charge ratio) around the targeted masses using a resolution of $R = 70{,}000$ (at m z^{-1} 200) after accumulation to a target value of $2e^5$ with a maximum allowed ion accumulation time of 200 ms. The tMS2 scans were conducted for each target using higher energy collision induced dissociation (HCD) at a target value of $2e^5$ and a resolution $R = 35{,}000$ with an isolation window of m $z^{-1} = 2$ without offset with maximum allowed ion accumulation of 200 ms. The lock mass option was enabled for internal recalibration during the analysis.

For the LC-MS analysis, the data were acquired using Xcalibur v2.5.5 and raw files were processed to generate peak list in Mascot generic format (*.mgf) using ProteoWizard release version 3.0.331. Database searches were performed using Mascot in-house version 2.4.0 to search the SwissProt database (Human, 11.08.2015, 20,203 proteins) assuming the digestion enzyme trypsin, at maximum one missed cleavage site, fragment ion mass tolerance of 0.05 Da, parent ion tolerance of 10 ppm and oxidation of methionines, and acetylation of the protein N-terminus as variable modifications. Spectral libraries were generated in Skyline using the BiblioSpec algorithm from the results of the database searches of the raw data files prior to MS1 filtering. The isotopic import filter was set to three (M, M + 1 and M + 2). After the import, displays of chromatographic traces were visually controlled and in some cases peak picking was manually adjusted. The quantification was performed in three independent experiments on the precursor and transition level, using the three isotopes of the precursor and the five most intense y-ion transitions (y3-y7) of the peptide VSQYIEWLQK (M + + light: 647.3455 Da, M + + medium: 649.3581 Da, M + + heavy: 651.3526 Da).

2.6. Degradation studies

To examine whether the three FVII mutants were degraded by proteasomes or lysosomes, CHO-K1 cells were grown in SILAC DMEM light (L) medium until a minimum of three cell divisions were reached. Cells were seeded in 6-well plates, cultured in DMEM SILAC light (L) medium until 80% confluency and then transiently transfected with pcDNA3-FVIIwt, pcDNA3-p.G420V, pcDNA3-p.I289del, or pcDNA3-p.A354V-p.P464Hfs as described above. Four hours after transfection, light (L) medium was exchanged with heavy (H) medium for cells transfected with FVIIwt plasmid and with medium (M) medium for cells transfected with the FVII mutant plasmid. The cells were immediately treated with 10 µM lactacystin or 40 µM chloroquine (both Sigma-Aldrich) for 24 h. Untreated cells were used as control. Cells were harvested as for the pc-SILAC experiments and proteins were separated as described above. LC-MS experiments and analysis of the data were performed as described in the preceding paragraph.

To investigate possible involvement by other proteolytic systems, CHO-K1 cells stably expressing FVIIwt or the FVII mutants were incubated in DMEM medium supplemented with 1% FBS and 20 µg/mL of *N*-acetyl-Leu-Leu-Norleu-al ALLN (Sigma-Aldrich). After 6h the cells were lysed in RIPA buffer (Sigma-Aldrich) containing Halt protease and phosphatase inhibitor cocktail 1X (Thermo Fisher Scientific). FVIIAg was measured in cell lysates by ELISA as described in precedent paragraphs. Cells were also incubated in medium containing 1% dimethyl sulfoxide (DMSO Sigma-Aldrich).

2.7. Confocal immunofluorescence microscopy

CHO-K1 cells were seeded in 4-well Lab-Tek II chamber slides (Thermo Fisher Scientific) and cultured in DMEM (Lonza) supplemented with 10 µg/mL of Vitamin K1. At 80% confluency, cells were transfected with 0.5 µg of pcDNA3-FVIIwt, pcDNA3-p.G420V, pcDNA3-p.I289del, or pcDNA3-p.A354V-p.P464Hfs as described above. Immunostaining was performed 24 h after transfection with antibodies against FVII (Abcam, Cambridge, UK), the ER marker protein disulfide isomerase (PDI) (Enzo Life Sciences, Farmingdale, NY, USA) or the Golgi marker GM130 (BD Biosciences, San Jose, CA, USA). Alexa Fluor® 488 goat anti-rabbit (Cell Signaling, Carlsbad, CA, USA) and Alexa Fluor® 568 donkey anti-mouse (Thermo Fisher Scientific) were used as secondary antibodies. Cells were mounted in the SlowFade® Gold Antifade reagent with DAPI (Thermo Fisher Scientific) and analyzed using the laser scanning Zeiss LSM 710 confocal microscope (Carl Zeiss MicroImaging GmbH, Jena, Germany). The objectives used were a LD LCI Plan-Apochromat 25x/0.8 for oil, or a Plan-Apochromat 63x/1.40 Oil DIC M27 (both from Carl Zeiss MicroImaging GmbH, Jena, Germany). Image processing was performed with basic software ZEN 2011 (Carl Zeiss MicroImaging GmbH) and Photoshop CS4 Extended (Adobe, Mountain View, CA, USA). Negative controls using only secondary antibodies, as well as double negative controls using one of the primary antibodies and both secondary antibodies were included. The Manders' co-localization coefficient was calculated with the ZEN 2011 software, and describes the sum of intensities for co-localizing pixels in the respective channel, as compared to the overall sum of pixels above threshold. A threshold was set above the noise level for each chromophore. Pearson's correlation coefficient was calculated with the ZEN 2011 software and describes the correlation of the intensity distribution between channels. A value of 1 represents a strong positive correlation, 0 indicates no correlation and -1 represents a total negative correlation. Three independent experiments were performed.

2.8. Molecular modeling of FVIIp.G420V

Figures and the modeling were prepared with The PyMOL Molecular Graphics System, Version 1.8 Schrödinger, LLC [18] using the atomic coordinates from protein data bank entry 1DAN (PDB ID: 1DAN). The amino acid sequence for FVII (Uniprot identifier P08709-1) was used as input sequence and the p.G420V mutation was tested in the following online web tools: PolyPhen-2 [19], SIFT [20] and PROVEAN [21]. All three servers returned with confidently scores that point towards a disease causing mutation (PolyPhen-2 Score = 1, Provean score − 8.7).

2.9. Statistical analysis

The results were tested for statistical significance using one-way ANOVA or Student's *t*-Test. The two-way ANOVA test was used for pc-SILAC experiments. A P-value < 0.05 was considered statistically significant. Results are presented as mean ± SEM. GraphPad Prism 5 (GraphPad Software Inc., La Jolla, CA, USA) was used for statistical analysis.

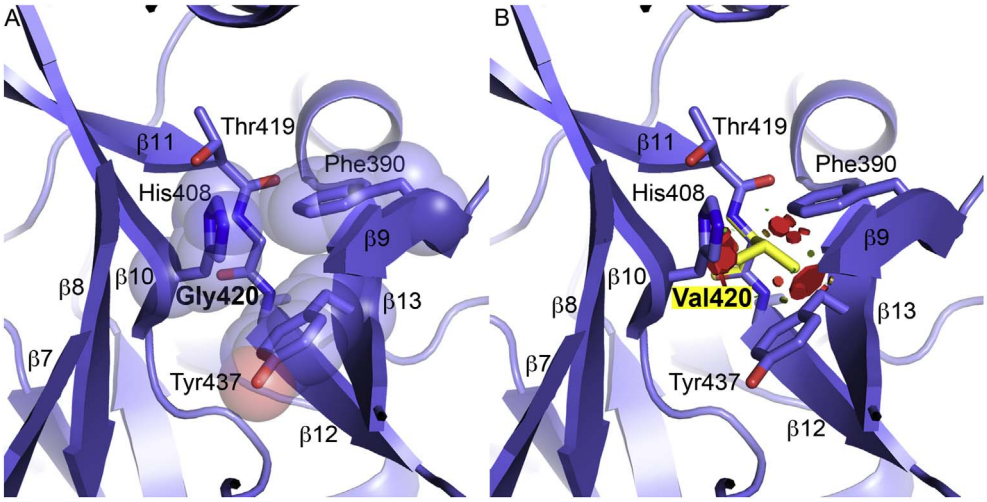

Fig. 1. Molecular modeling of p.G420V. (A) Cartoon representing the central β-sheet of FVII. Gly420 is shown as sticks and is found in a key position between β strand 11 and 12. Gly420 serves as a critical bridge point between the β-sheets 9, 12 and 13 and 7, 8, 10, and 11. The aromatic residues Phe330, His348 and Tyr377 (transparent spheres) form a tight hydrophobic core connecting the two β sheets. (B) Cartoon indicating the effect of substituting Gly420 with Val420.

3. Results

3.1. Molecular modeling of p.G420V predicted severe structural damage

Glycine 420 is numbered G211 in the activated FVII crystal structure with the PDB ID: 1DAN. The mutation is found in a key position of the FVII core structure, i.e. the region between two β-barrels forming the core structure of FVII. Glycine 420 acts as the strand-breaking residue between strand 11 and 12. Since no hydrogen binding networks required in a β-sheet are allowed by the adopted G420 conformation, the two β-sheets formed by strands 7 and 8, 10 and 11 and strands 9, 12 and 13 will be effectively separated (Fig. 1A and B). The glycine residue adopts a trans-conformation and is fixed in a planar conformation. No other amino acid is able to adopt such a conformation. It is therefore likely that a mutation of glycine to valine will cause a severe structural disruption and thus introduce a certain degree of misfolding or a destabilization of FVII that might lead to a reduction of FVII present in the blood stream. The p.G420V variant was also tested using the in silico mutation prediction tools PolyPhen-2 and PROVEAN and it was predicted as probably disease damaging or deleterious by both programs. The SIFT tool predicted that only the amino acid glycine (G) would be tolerated in the tested position.

The one residue-deletion p.I289del was not modeled because being a deletion, no template structural model to model against is available. The extension generated by p.A354V-p.P464Hfs does not produce a polypeptide chain that resembles any known structure.

3.2. Impaired secretion of FVII mutants

In order to investigate the effects of the p.I289del, p.A354V-p.P464Hfs and p.G420V mutations on the synthesis and secretion of FVII, CHO-K1 cells were transiently transfected with the expression vectors for the FVII variants as well as wild-type FVII for comparison. The FVIIAg levels were measured in the cell lysates and culture medium 24 h post transfection. The mean recombinant (r) FVIIwt protein level in the medium was 0.06 mU/μg of total protein in the corresponding cell lysates (± 0.01), whereas the levels of rFVII-289del, rFVII-354V-464Hfs or rFVII-420V were below the limit of detection. The results indicated that the mutations affected the secretion of FVII. A slight decrease in the intracellular levels of rFVII-289del and rFVII-354V-464Hfs when compared to the rFVIIwt was observed in the cell lysates, however, these differences did not reach significance ($p = 0.3$). Intracellular levels of rFVII-420V were similar to the rFVIIwt levels (Fig. 2). Non-transfected CHO-K1 cells were used as a negative control and no detectable levels of FVII were observed in neither cell lysates nor culture medium (data not shown). FVII activity was investigated in the culture medium by chromogenic assay. FVII activity of the three mutants was under the limit of detection.

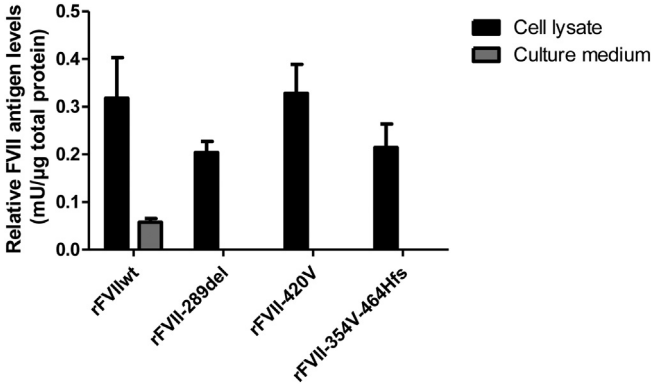

Fig. 2. FVII protein levels in cell lysates and culture medium of CHO-K1 cells transiently expressing FVIIwt, or the FVII mutants. CHO-K1 cells were transiently transfected with plasmid constructs expressing FVIIwt or the three FVII variants: p.I289del, p.G420V and p.A354V-p.P464Hfs. FVII protein levels (mU) were measured in the cell lysates and culture medium 24 h post transfection. The total concentration of FVII was adjusted to the total protein concentration in the corresponding cell lysates. Results from three independent experiments in duplicates are presented as Mean ± SEM. (One-way ANOVA test rFVIIwt versus rFVII-289del, rFVII-420V and rFVII-354V-464Hfs. $p = 0.3$ in cell lysates).

In order to examine whether the reduced secretion of the FVII mutants was due to differences in the mRNA steady state levels, the mRNA levels of FVIIwt and the three FVII mutants were determined by qRT-PCR. As shown in Fig. 3 no significant differences in the FVII mRNA levels were detected between the three FVII mutants and the FVIIwt ($p = 0.13$).

3.3. The synthesis of the FVII mutants is delayed and reduced

Since the secretion of the three FVII mutants was impaired, their synthesis was further investigated by pc-SILAC. The percentages (%) of peak contribution of the light (L), medium (M) and heavy (H) were calculated assuming the summed signal of light (L), medium (M) and heavy (H) being 100%. Medium (M) corresponds to the FVII mutants and heavy (H) to the rFVIIwt. As shown in Fig. 4A–C, the synthesis rates of the three FVII mutants (M) were slower and significantly reduced compared to rFVIIwt (H) at the start of the chase (time 0, 1, and 2 h after the medium exchange). After 4 h, the synthesis of the three mutants (M) increased, whereas the levels of rFVIIwt (H) started to decrease as the protein was secreted into the medium. At 24 h chase, the levels of the three FVII mutants continued to increase being more

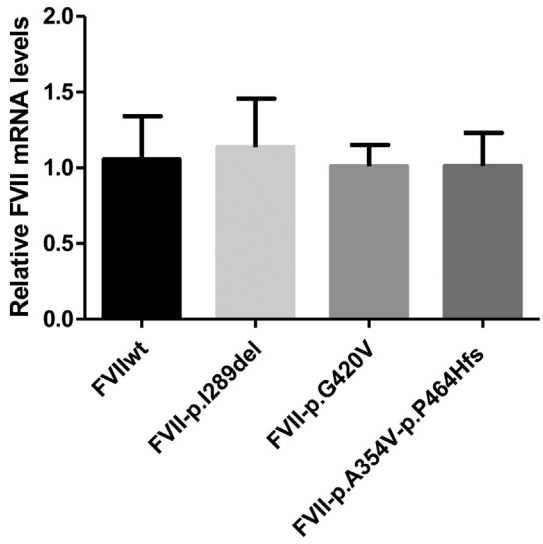

Fig. 3. mRNA levels of FVIIwt and FVII mutants. CHO-K1 cells were transiently transfected with plasmid constructs expressing FVIIwt or the three FVII variants: p.I289del, p.G420V and p.A354V-p.P464Hfs. mRNA was isolated 24 h post transfection. FVII mRNA levels were determined using quantitative RT-PCR with TBP as endogenous control. The results are presented as mean of the fold-change expression of the F7 gene. Results from three independent experiments are presented as Mean ± SEM (One-way ANOVA test comparing mRNA of FVII mutants vs mRNA levels of FVIIwt $p = 0.13$).

evident for the rFVII-289del, which overlapped the levels of rFVIIwt. After 24 h, the levels of rFVIIwt were approximately 40 to 60% of the values at time 0. These results indicate that the synthesis rate of the FVII mutants was altered by being delayed in time and also suggest that these mutant proteins were retained in the cell.

3.4. Degradation of FVII

Since the expression studies showed an impaired secretion of the three FVII mutants, we next examined whether intracellular degradation of these mutant proteins could be involved. CHO-K1 cells transiently transfected with the pcDNA3-FVIIwt, pcDNA3-p.G420V, pcDNA3-p.I289del, or pcDNA3-p.A354V-p.P464Hfs constructs were treated for 24 h with the proteasomal or lysosomal inhibitors lactacystin and chloroquine, respectively, followed by SILAC analysis. Only non-significant changes ($p > 0.05$) in the mutant FVII protein levels were detected by SILAC in the cell lysates after treatment with lactacystin or chloroquine for 24 h (data not shown). Therefore, differences in degradation by proteasomes or lysosomes were undetectable for the mutant proteins.

We next investigated the possible degradation of the FVII mutants by other proteolytic systems. CHO-K1 cells stably expressing FVIIwt or the FVII mutants were treated for 6 h with ALLN, an inhibitor of cysteine proteases, calpain and the 26S ubiquitin-proteasome. FVII protein levels were measured in the cell lysates by ELISA. No differences were observed in the FVII levels of the three FVII mutant proteins treated with ALLN when compared with untreated cells. A slight significant increase of FVII protein levels was observed in the cells expressing FVIIwt after treatment with ALLN (data not shown).

3.5. Intracellular localization of FVII

Since the FVII mutants showed impaired secretion and no evidence of degradation, we next assessed their intracellular localization using confocal immunofluorescence microscopy by staining cells transiently transfected with expression vectors for FVII variants with antibodies against FVII and either the ER marker PDI or the Golgi marker GM130. As shown in Fig. 5A, the rFVIIwt and rFVII mutants co-localized with PDI. However, only rFVIIwt co-localized with GM130 (Fig. 5B). The negative control using only the secondary antibodies did not show any staining (data not shown). The double negative controls using one of the primary antibodies (FVII or PDI or GM130) and the two secondary antibodies (goat anti-rabbit and donkey anti-mouse) did not reveal any cross-reaction (data not shown). The Manders' co-localization coefficient and the Pearson's correlation coefficient in Golgi were calculated. Manders' co-localization coefficient was significantly decreased in the rFVII mutants compared to rFVIIwt (Fig. 5C). The Pearson's correlation coefficient in Golgi was negative in the rFVII mutants (Fig. 5D). These results indicate that the mutant FVII proteins were predominantly localized in the ER and evoked a defective transport of the proteins from the ER to the Golgi.

4. Discussion

The aim of the present study was to investigate the molecular mechanisms responsible for FVII deficiency caused by three different types of mutations (missense, deletion and elongation) in the *F7* gene, all affecting the catalytic domain of FVII and associated with a different degree of severity.

The p.G420V substitution is associated with undetectable FVII protein levels in plasma and severe bleeding [7]. The double missense mutation-single deletion p.A354V-p.P464Hfs resulting in an elongated protein is frequently observed in individuals from Central Europe. It is clinically heterogeneous with symptoms ranging from asymptomatic to severe bleeding and not strictly related to the levels of FVIIc [1,3]. The p.I289del was found in a patient from Thailand who presented severe intra-cranial hemorrhage at birth (Pinotti M, Chuansumrit A unpublished). Interestingly, for one of them (p.G420V) molecular modeling was able to predict a severe structural disruption, which further supports the expression studies.

In the present study, transiently transfected CHO-K1 cells were used to explore the mechanisms by which these three different mutations reduce the levels of FVII. We found impaired secretion of the mutants with undetectable levels of FVII in the culture medium. These results correlated with the very reduced FVII levels measured in patients carrying these mutations. The p.G420V produces undetectable levels of FVII in plasma and it has been reported by Rizzotto et al. in a cellular model that the protein level and the activity of rFVII-420V were undetectable in the culture medium [7]. The only known patient carrying the p.I289del had undetectable levels of FVII in plasma. In patients carrying the combined mutation p.A354V-p.P464Hfs, the FVII levels are very low with a median of FVIIAg (%) of 1.9 [1]. Using pc-SILAC, which enables the determination of relative levels of two conditions for newly synthesized proteins at different time points as well as the level of remaining preexisting protein levels [22], we demonstrated that the synthesis rate of all mutant FVII proteins was delayed compared to rFVIIwt with accumulation of the mutant proteins within the cell. Confocal immunofluorescence microscopy revealed retention of all FVII mutants in ER without reaching Golgi, suggesting a folding defect of the mutant proteins affecting their normal trafficking. In spite of potential differences suggested by the quite different mutation types, at the protein levels all mutants appeared to share a common altered pathway.

Folding of proteins is essential to acquire their functional three-dimensional (3D) structure. The major folding occurs in the cytoplasm or in specific compartments, such as the mitochondria or the ER [23,24]. When a misfolded protein transiently accumulates in the ER, the ER can increase its capacity to handle misfolded proteins via the unfolded protein response (UPR). Additionally, it can activate the ER associated degradation (ERAD) that identifies and destroys individual irreversibly misfolded proteins through the ubiquitin-proteasome system [11,13,25,26]. Since no significant changes in protein levels of the three FVII variants were detected after treatment with the proteasomal and lysosomal inhibitors lactacystin and chloroquine, respectively, no evidence for degradation/ERAD was observed. This suggests that the

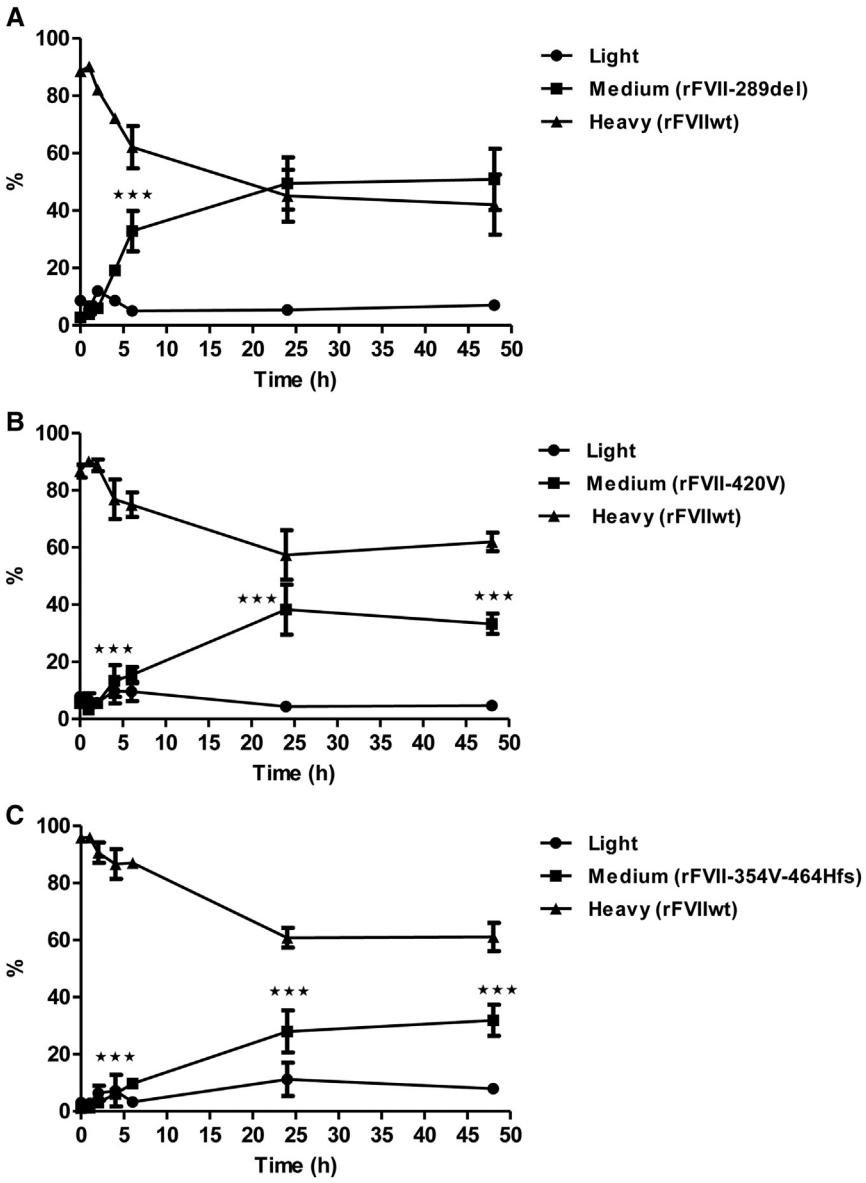

Fig. 4. Synthesis of FVIIwt and FVII mutants in transiently transfected CHO-K1 cells. CHO-K1 cells transiently expressing rFVIIwt, rFVII-289del, rFVII-420V, or rFVII-354 V-464Hfs were switched to heavy (H, FVIIwt) or medium (M, FVII mutants) DMEM and cell lysates were collected at 0, 1, 2, 4, 6, 24 and 48 h after medium exchange. The cell lysates from H and M were then mixed at equal proportions. The sum of all peak areas of the light (L), medium (M) and heavy (H) signals result in 100% signal, distributed between the three labels. The contribution of each label was calculated out of ratios light to medium (L/M) and heavy to medium (H/M) and presented in percent. Heavy corresponds to the rFVIIwt protein and medium to the mutants rFVII-289del (A), rFVII-420V (B) or rFVII-354V-464Hfs (C). Results of three independent experiments are presented (Two-way ANOVA test rFVIIwt vs rFVII-289del $***p < 0.001$, rFVIIwt vs rFVII-420V $***p < 0.001$ and rFVIIwt vs rFVII-354V-464Hfs $***p < 0.001$).

FVII mutants were retained in ER, presumably associated with folding enzymes/chaperones assisting in the correction of their abnormal folding. Degradation of misfolded proteins by other proteolytic pathways like serine and cysteine proteases has been reported [27]. We did not observed changes in the protein levels of the three FVII variants when cells were treated with the combined inhibitor of cysteine protease, calpain and proteasome ALLN indicating that degradation of the FVII mutants by other proteolytic system was not detectable in our cell model.

Protein misfolding has been described in other coagulation factor deficiencies. For mutations causing protein C (PC) deficiency, proteasomal degradation of the mutant protein has been reported [17], whereas in another report, a defective trafficking of a mutant PC caused ER stress and induced UPR [28,29]. For two mutations in the EGF-like domain of the *F9* gene, it was reported that the mutant proteins were retained in ER associated with the chaperone calreticulin and that the proteins were degraded by cysteine proteases [30]. Molecular studies on a FVIII mutation (N1922S) resulting in moderate to severe hemophilia, demonstrated a domain specific folding defect with poor secretion of the protein and impaired transit from ER to the Golgi [31]. Rizzoto et al. reported two FVII variants (L-48P and L-42P), which showed impaired targeting to ER [7]. In their study, they also demonstrated that the rFVII-420V variant was retained within the cells, being accumulated in ER. This observation is in concordance with our findings for rFVII-420V.

In conclusion, the present study demonstrates that different types of mutations, which are all located in the catalytic domain of FVII, result in impaired secretion. This is in accordance with the very low plasma levels observed in patients with these FVII mutants. The results indicate that abnormal folding of the proteins causing ineffective trafficking from the ER to the Golgi and accumulation in the ER are likely a common mechanism responsible for the reduced secretion of FVII in genetically-determined pathologic conditions.

Transparency document

The Transparency document associated with this article can be found, in online version.

Acknowledgments

The authors thank Margarita Strozynski for her valuable help with the sample preparation for mass spectrometry analysis. We also thank Marie-Christine Mowinckel for technical assistance with ELISA.

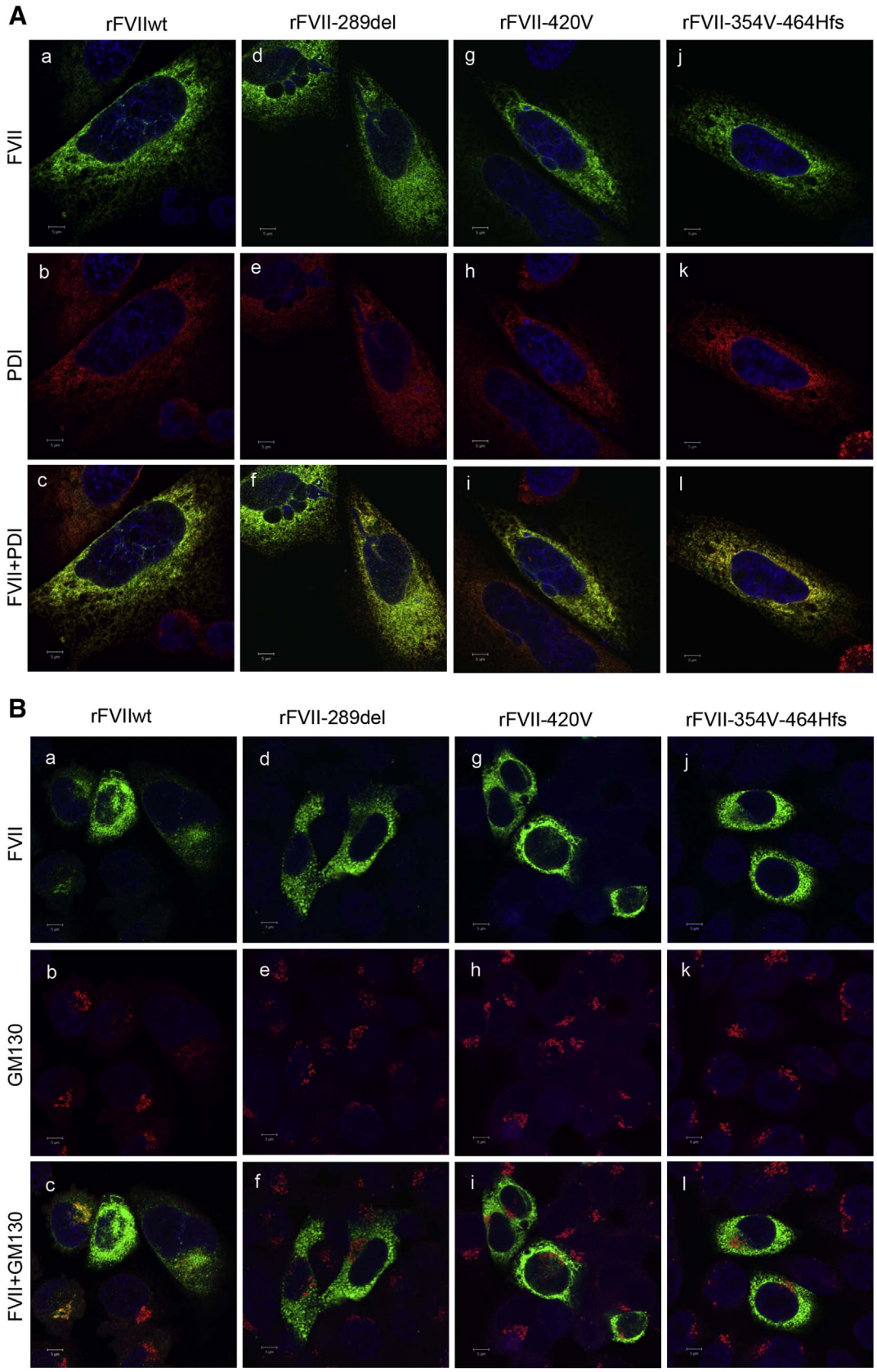

Fig. 5. Intracellular localization of rFVIIwt and rFVII-289del, rFVII-420V and rFVII-354V-464Hfs. Confocal images from FVII (green) and PDI (red)-stained (A), FVII (green) and GM130 (red)-stained (B), CHO-K1 cells transiently transfected with FVIIwt, p.I289del, p.G420V or p.A354V-p.P464Hfs. (A) Cells were stained with antibodies against FVII (a, d, g, j), and PDI (b, e, h, k) and merged images of green and red are shown in c, f, i, l. Co-localized green and red pixels are shown in yellow color. (B) Cells were stained with antibody against FVII (a, d, g, j) and GM130 (b, e, h, k), and merged images are shown in c, f, i, l. Three independent experiments were performed. Bar 5 μm. (C–D) The co-localization of FVII with GM130 was calculated based on the merged c, f, i, l images in B by the Manders' co-localization coefficient and the Pearson's correlation coefficient. Results are presented statistically as the mean ± SEM of at least three independent experiments (One-way ANOVA comparing cells expressing FVII mutants to cells expressing rFVIIwt in the FVII/GM130-stained samples. ((**) $p < 0.005$ (*) $p < 0.05$).

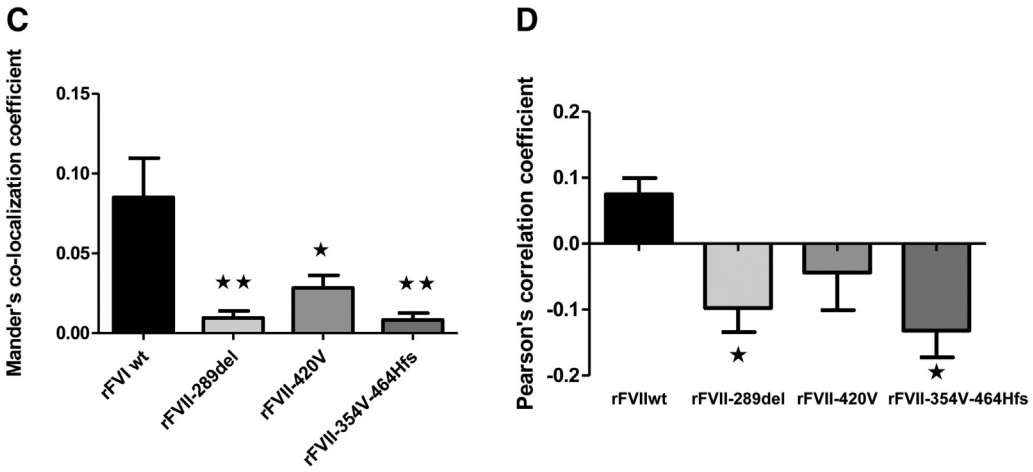

Fig. 5. (*continued*)

Funding

The study was supported by grants from the South-Eastern Norway Health Authority, Hamar, Norway.

Disclosure of conflict of interest

The authors declare that they do not have conflict of interest.

References

[1] G. Mariani, F.H. Herrmann, A. Dolce, A. Batorova, D. Etro, F. Peyvandi, K. Wulff, J.F. Schved, G. Auerswald, J. Ingerslev, F. Bernardi, Clinical phenotypes and factor VII genotype in congenital factor VII deficiency, Thromb. Haemost. 93 (2005) 481–487.
[2] D.J. Perry, V.I.I. Factor, Deficiency, Br. J. Haematol. 118 (2002) 689–700.
[3] G. Mariani, F. Bernardi, Factor VII deficiency, Semin. Thromb. Hemost. 35 (2009) 400–406.
[4] R. Palla, F. Peyvandi, A.D. Shapiro, Rare bleeding disorders: diagnosis and treatment, Blood 125 (2015) 2052–2061.
[5] J.H. Mcvey, E. Boswell, A.D. Mumford, G. Kemball-Cook, E.G. Tuddenham, Factor VII deficiency and the FVII mutation database, Hum. Mutat. 17 (2001) 3–17.
[6] M. Hunault, A.A. Arbini, J.A. Carew, F. Peyvandi, K.A. Bauer, Characterization of two naturally occurring mutations in the second epidermal growth factor-like domain of factor VII, Blood 93 (1999) 1237–1244.
[7] L. Rizzotto, M. Pinotti, P. Pinton, R. Rizzuto, F. Bernardi, Intracellular evaluation of ER targeting elucidates a mild form of inherited coagulation deficiency, Mol. Med. 12 (2006) 137–142.
[8] K. Suzuki, T. Sugawara, Y. Ishida, A. Suwabe, Compound heterozygous mutations (p.Leu13Pro and p.Tyr294*) associated with factor VII deficiency cause impaired secretion through ineffective translocation and extensive intracellular degradation of factor VII, Thromb. Res. 131 (2013) 16672.
[9] R. Tanaka, D. Nakashima, A. Suzuki, Y. Miyawaki, Y. Fujimori, T. Yamada, A. Takagi, T. Murate, K. Yamamoto, A. Katsumi, T. Matsushita, T. Naoe, T. Kojima, Impaired secretion of carboxyl-terminal truncated factor VII due to an F7 nonsense mutation associated with FVII deficiency, Thromb. Res. 125 (2010) 262–266.
[10] C.J. Guerriero, J.L. Brodsky, The delicate balance between secreted protein folding and endoplasmic reticulum-associated degradation in human physiology, Physiol. Rev. 92 (2012) 537–576.
[11] J.E. Chambers, S.J. Marciniak, Cellular mechanisms of endoplasmic reticulum stress signaling in health and disease. 2. Protein misfolding and ER stress, Am. J. Phys. Cell Physiol. 307 (2014) C657–70.
[12] M. Schroder, R.J. Kaufman, The mammalian unfolded protein response, Annu. Rev. Biochem. 74 (2005) 739–789.
[13] J.L. Brodsky, W.R. Skach, Protein folding and quality control in the endoplasmic reticulum: recent lessons from yeast and mammalian cell systems, Curr. Opin. Cell Biol. 23 (2011) 464–475.
[14] T.K. Chaudhuri, S. Paul, Protein-misfolding diseases and chaperone-based therapeutic approaches, FEBS J. 273 (2006) 1331–1349.
[15] T. Yamazaki, G.A. Nicolaes, K.W. Sorensen, B. Dahlback, Molecular basis of quantitative factor V deficiency associated with factor V R2 haplotype, Blood 100 (2002) 2515–2521.
[16] H. Mikkola, L. Muszbek, G. Haramura, E. Hamalainen, A. Jalanko, A. Palotie, Molecular mechanisms of mutations in factor XIII A-subunit deficiency: in vitro expression in COS-cells demonstrates intracellular degradation of the mutant proteins, Thromb. Haemost. 77 (1997) 1068–1072.
[17] M. Nishio, T. Koyama, M. Nakahara, N. Egawa, S. Hirosawa, Proteasome degradation of protein C and plasmin inhibitor mutants, Thromb. Haemost. 100 (2008) 405–412.
[18] H. Dou, L. Buetow, G.J. Sibbet, K. Cameron, D.T. Huang, BIRC7-E2 ubiquitin conjugate structure reveals the mechanism of ubiquitin transfer by a RING dimer, Nat. Struct. Mol. Biol. 19 (2012) 876–883.
[19] I. Adzhubei, D.M. Jordan, S.R. Sunyaev, Predicting functional effect of human missense mutations using PolyPhen-2, Curr. Protoc. Hum. Genet. (2013) (Supplement 76, 7.20.1-41).
[20] R. Vaser, S. Adusumalli, S.N. Leng, M. Sikic, P.C. Ng, SIFT missense predictions for genomes, Nat. Protoc. 11 (2016) 1–9.
[21] Y. Choi, A.P. Chan, PROVEAN web server: a tool to predict the functional effect of amino acid substitutions and indels, Bioinformatics 31 (2015) 2745–2747.
[22] I. Fierro-Monti, J. Racle, C. Hernandez, P. Waridel, V. Hatzimanikatis, M. Quadroni, A novel pulse-chase SILAC strategy measures changes in protein decay and synthesis rates induced by perturbation of proteostasis with an Hsp90 inhibitor, PLoS One 8 (2013) e80423.
[23] C.M. Gomes, Protein misfolding in disease and small molecule therapies, Curr. Top. Med. Chem. 12 (2012) 2460–2469.
[24] Y.E. Kim, M.S. Hipp, A. Bracher, M. Hayer-Hartl, F.U. Hartl, Molecular chaperone functions in protein folding and proteostasis, Annu. Rev. Biochem. 82 (2013) 323–355.
[25] I. Braakman, D.N. Hebert, Protein folding in the endoplasmic reticulum, Cold Spring Harb. Perspect. Biol. 5 (2013) a013201.
[26] F.U. Hartl, A. Bracher, M. Hayer-Hartl, Molecular chaperones in protein folding and proteostasis, Nature 475 (2011) 324–332.
[27] L. Fayadat, S. Siffroi-Fernandez, J. Lanet, J.L. Franc, Degradation of human thyroperoxidase in the endoplasmic reticulum involves two different pathways depending on the folding state of the protein, J. Biol. Chem. 275 (2000) 15948–15954.
[28] L. Tjeldhorn, N. Iversen, K. Sandvig, J. Bergan, P.M. Sandset, G. Skretting, Protein C mutation (A267T) results in ER retention and unfolded protein response activation, PLoS One 6 (2011) e24009.
[29] L. Tjeldhorn, N. Iversen, K. Sandvig, J. Bergan, P.M. Sandset, G. Skretting, Functional characterization of the protein C A267T mutation: evidence for impaired secretion due to defective intracellular transport, BMC Cell Biol. 11 (2010) 67.
[30] N. Enjolras, J.L. Plantier, M.H. Rodriguez, M. Rea, O. Attali, C. Vinciguerra, C. Negrier, Two novel mutations in EGF-like domains of human factor IX dramatically impair intracellular processing and secretion, J. Thromb. Haemost. 2 (2004) 1143–1154.
[31] R.J. Summers, S.L. Meeks, J.F. Healey, H.C. Brown, E.T. Parker, C.L. Kempton, C.B. Doering, P. Lollar, Factor VIII A3 domain substitution N1922S results in hemophilia A due to domain-specific misfolding and hyposecretion of functional protein, Blood 117 (2011) 3190–3198.